

Pre-Eocene Arabia-Eurasia collision: New constraints from the Zagros Mountains (Amiran Basin, Iran)

Gaoyuan Sun¹, Xiumian Hu^{2,*}, Eduardo Garzanti³, Marcelle K. BouDagher-Fadel⁴, Yiwei Xu², Jingxin Jiang², Erik Wolfgring⁵, Yasu Wang¹, and Shijun Jiang¹

¹College of Oceanography, Hohai University, Nanjing 210024, China

²State Key Laboratory for Mineral Deposits Research, School of Earth Sciences and Engineering, Nanjing University, Nanjing 210023, China

³Department of Earth and Environmental Sciences, Università di Milano-Bicocca, 20126 Milan, Italy

⁴Department of Earth Sciences, University College London, London WC1H 0BT, UK

⁵Dipartimento di Scienze della Terra, Università degli Studi di Milano, Via Mangiagalli 34, 20133 Milan, Italy

ABSTRACT

The timing of continental collision between Arabia and Eurasia is a highly controversial issue, on which new constraints are here provided from the Amiran Basin (Zagros Mountains, Iran). Upper Cretaceous carbonate ramps grown along the Arabian northern margin are overlain by the siliciclastic deep-water Amiran and shallow-water Kashkan Formations, dated biostratigraphically as 64–60 Ma (Paleocene) and 56–52 Ma (earliest Eocene), respectively. Abundant ophioliticlastics, detrital Cr-spinel geochemistry, and detrital zircons with positive $\epsilon_{\text{Hf}}(t)$ values dated as 110–80 Ma, 180–160 Ma, and 260–200 Ma indicate that the Amiran Formation was derived from the obducted Kermanshah ophiolite and Sanandaj-Sirjan zone. Besides sharing similar composition and zircon-age spectra, the overlying Kashkan Formation contains recycled detritus and one new zircon-age component with negative $\epsilon_{\text{Hf}}(t)$ values dated as 250–200 Ma, suggesting supply from additional sources in Central Iran. The Amiran Formation thus indicates that the Kermanshah ophiolite, obducted in the Late Cretaceous, was subaerially exposed to erosion in the Paleocene. The Kashkan Formation testifies to the establishment of a new fluvial system, sourced from Central Iran and flowing across the Zagros suture zone. This implies that continental collision between Arabia and Eurasia took place before the beginning of the Eocene (56 Ma) in the Lorestan region (Iran).

INTRODUCTION

The sequence of tectonic events that led to the final closure of the Neotethys Ocean has remained poorly constrained and particularly controversial in the Middle East, where Late Cretaceous ophiolite obduction recorded all along the Arabian continental margin from Syria to Oman was followed by collision with Eurasia and formation of the Zagros orogen (Alavi, 1994, 2004; Agard et al., 2011). The geodynamic and paleogeographic evolution of the Middle East cannot be properly understood

until the controversy concerning the onset of Arabia-Eurasia continental collision is resolved.


Estimates of Arabia-Eurasia collision timing along the Zagros suture vary widely from as early as Late Cretaceous to as late as Pliocene (e.g., Alavi, 1994; McQuarrie and van Hinsbergen, 2013; Zhang et al., 2017; Koshnaw et al., 2018; Cai et al., 2021; GholamiZadeh et al., 2022). Such a large uncertainty reflects the complexity of the probably multistep tectonic evolution in this area, which has been explained by different models involving successive phases of ophiolite obduction and island-arc or micro-continent collision. A preferred collision time of the latest Eocene–Oligocene is based mainly on plate kinematic reconstructions (e.g., McQuarrie and van Hinsbergen, 2013); nevertheless, the varied estimates of crustal deformation and post-collisional convergence in the Zagros would limit this collision timing assessment


(e.g., Hatzfeld and Molnar, 2010; Pirouz et al., 2017). Provenance studies conducted along the Zagros orogen from the Iraqi Kurdistan to Lorestan and Fars in Iran have suggested a ca. 36–26 Ma minimum age for collision onset based on the sedimentary arrival in Arabia of detritus from Iran at this time (Koshnaw et al., 2018, 2021; Cai et al., 2021; GholamiZadeh et al., 2022). These studies, however, are based on discontinuous stratigraphic successions and provide only a minimum age for collision (e.g., Koshnaw et al., 2018).

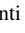
A continuous sedimentary sequence is needed to more firmly constrain the timing of collision onset and its relationships with Late Cretaceous ophiolite obduction. This is the aim of the present study, which integrates high-resolution biostratigraphy, sandstone petrography, detrital Cr-spinel geochemistry, and detrital-zircon U-Pb age and Hf isotope data on the Upper Cretaceous to Miocene sedimentary sequence continuously exposed in the Amiran Basin of the Lorestan region (southwestern Iran). These results shed new light on the orogenic evolution of the Zagros Mountains.

GEOLOGICAL SETTING

The northwest-southeast-trending Zagros orogen is the consequence of the closure of the Neotethys Ocean and Arabia-Eurasia continental collision (Fig. 1A; Alavi, 1994). Central Iran, located to the north of the Zagros Mountains, chiefly consists of metamorphic and magmatic rocks overlain by Jurassic–Paleogene sedimentary successions (Agard et al., 2011). The orogen can be subdivided into three major sub-parallel tectonic domains (northeast to southwest): the Urumieh-Dokhtar magmatic arc,

Gaoyuan Sun  <https://orcid.org/0000-0002-0914-0398>

Xiumian Hu  <https://orcid.org/0000-0002-5401-8682>

Eduardo Garzanti  <https://orcid.org/0000-0002-8638-9322>
*huxm@nju.edu.cn

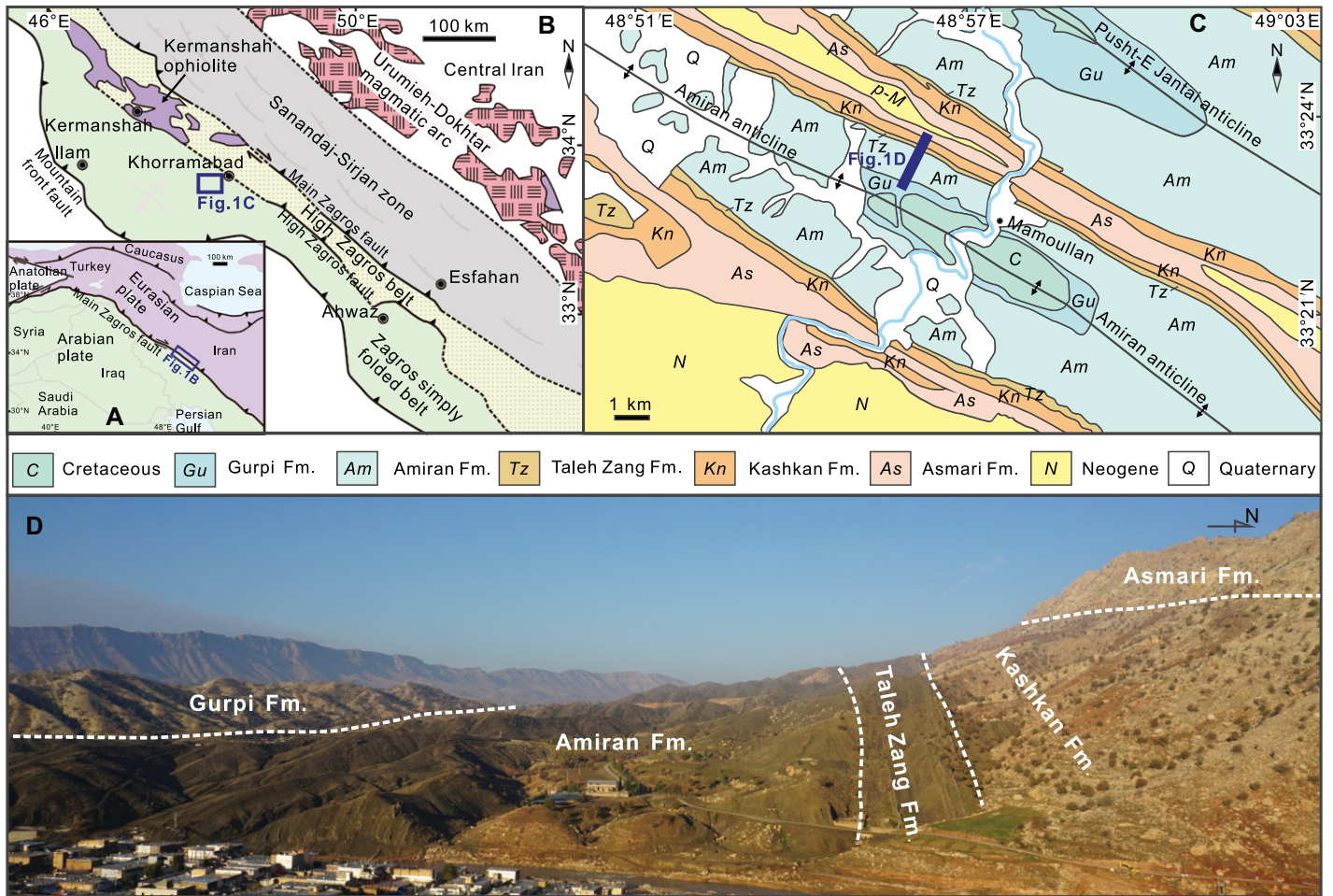


Figure 1. Geology of the study area. (A) Tectonic boundary between Arabia and Eurasia marked by the Main Zagros fault. (B) Structural map of the Zagros belt in Iran (after Homke et al., 2009). (C) Geological map of the Amiran Basin in Lorestan (after the 1:100,000-scale geological map of Pul-e Dukhtar in Takin et al. [1970]). (D) Panorama of Upper Cretaceous–Oligocene strata exposed in the Mamoullan section.

the Sanandaj-Sirjan zone, and the Zagros fold-thrust belt (Fig. 1B; Alavi, 2004). The Urumieh-Dokhtar magmatic arc, a linear magmatic belt along the southern border of Central Iran, is composed mostly of Eocene–Oligocene (55–25 Ma) plutonic and volcano-sedimentary rocks (Chiu et al., 2013). The Sanandaj-Sirjan zone consists mainly of metamorphosed and complexly deformed strata with Middle–Late Jurassic (180–150 Ma) and Paleogene (60–30 Ma) granitoids (Zhang et al., 2018). The Zagros fold-thrust belt, delimited to the north by the Main Zagros fault (Fig. 1B), includes the High Zagros belt and the Zagros simply folded belt (Fig. 1B; Alavi, 1994). The High Zagros belt contains ophiolite-radiolarite complexes (e.g., Kermanshah ophiolite) and Mesozoic–Cenozoic magmatic and sedimentary rocks (Agard et al., 2011). The Zagros simply folded belt consists mostly of mildly deformed Paleozoic–Mesozoic strata originally deposited onto Arabian basement (Alavi, 2004).

The Amiran Basin is located in the Zagros simply folded belt south of the Kermanshah ophiolite (Fig. 1B). Particularly well exposed in the Mamoullan section are thousands of

meters of Upper Cretaceous to Oligocene siliciclastic and carbonate strata distinguished into the Gurpi, Amiran, Taleh Zang, Kashkan, and Asmari Formations (Figs. 1C–1D). The Upper Cretaceous–lower Paleocene Gurpi Formation mostly consists of hemipelagic marlstone with intercalated wackestone, conformably overlain by the Paleogene Amiran Formation consisting of deep-water sandstone with intercalated mudrock. The upper Paleocene to lower Eocene Taleh Zang Formation comprises shallow-water foraminiferal limestone, overlain by the Eocene Kashkan Formation consisting of green and red fluvio-deltaic sandstone, conglomerate, and mudrock, unconformably capped in turn by the Oligocene Asmari Formation composed of shallow-marine dolostone and limestone (Homke et al., 2009; Saura et al., 2011).

METHODS

Biostratigraphic analyses based on foraminifera and calcareous nannofossils were conducted on 152 carbonates and 48 marlstones from the Mamoullan section. Clast point counts of 29 sandstones from the Amiran and Kashkan Formations were based on the Gazzi-Dickinson

method (Ingersoll et al., 1984). Detrital zircons from 14 sandstone samples yielded 1138 concordant U–Pb ages; 204 zircon grains dated as <350 Ma were analyzed for Hf isotopes. Cathodoluminescence (CL) images were taken of the Permo-Triassic zircons from the Kashkan Formation. The geochemistry of detrital Cr-spinels from four medium-grained Amiran sandstones was also analyzed. Analytical procedures and results are presented in the Supplemental Material¹.

BIOSTRATIGRAPHY OF THE AMIRAN BASIN

The identified species of benthonic and planktonic foraminifera and of calcareous nannofossils are referred to Huber et al. (2016), BouDagher-Fadel (2018), and Agnini et al. (2014), summarized in Figure 2 and provided as Figure S1 in the Supplemental Material.

¹Supplemental Material. Supporting figures, analytical methods, and data for provided in this study. Please visit <https://doi.org/10.1130/GEOL.S.23706384> to access the supplemental material, and contact editing@geosociety.org with any questions.

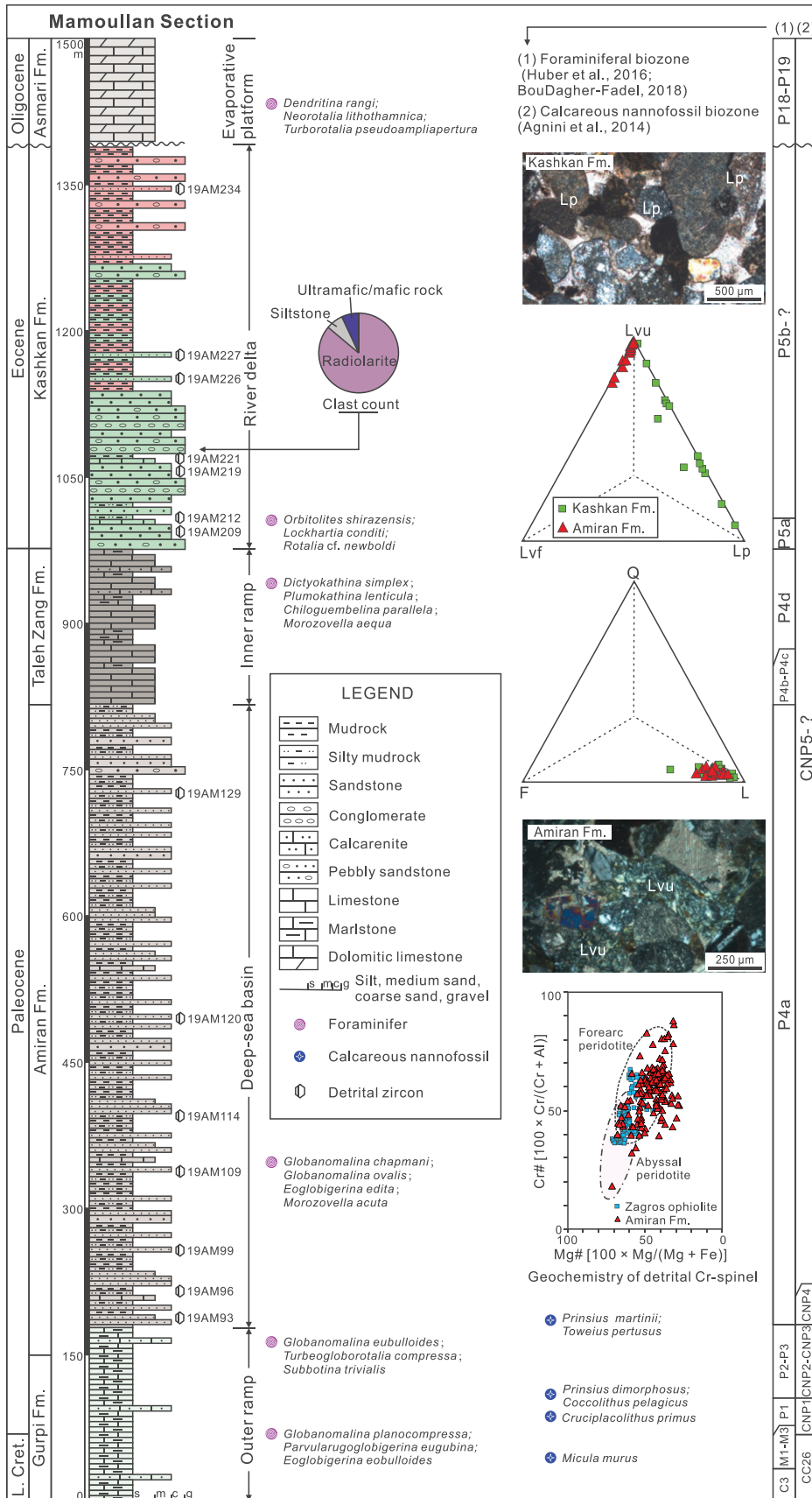


Figure 2. Stratigraphy of the Mamoullan section with key foraminifera and nannofossil assemblages. Stratigraphic column colors indicate the hues of the outcrops. Pie chart depicts percentages of clast types in Kashkan conglomerates; triangular diagrams summarize petrographic features of lithic to feldspathic lithic Amiran and Kashkan sandstones. Q—quartz; F—feldspars; L—lithics (Lvu—mafic volcanic and ultramafic; Lv—felsic volcanic; Lp—pelitic). Microphotographs of Amiran and Kashkan sandstones. Compositional fields of detrital Cr-spinels in the Amiran Formation after Dick and Bullen (1984); data on Zagros ophiolites from Moghadam and Stern (2015).

Campanian. The overlying strata yielded the Maastrichtian planktonic foraminifera *Racemiguembelina fructicosa*, *Contusotruncana contusa*, and *Abathomphalus mayaroensis*. In sample 19AM41 from the middle Gurpi Formation, *Globanomalina planocompressa*, *Parvarugoglobigerina eugubina*, and *Eoglobigerina eubulloides* indicate biozone P1a (ca. 64 Ma, Danian). This is consistent with the nannofossil assemblage found in samples 19AM30 and 19AM46, including *Cruciplacolithus primus*, *Prinsius dimorphosus*, and *Coccolithus pelagicus* (≥ 63 Ma). *Globanomalina eubulloides*, *Turbeogloborotalia compressa*, and *Subbotina trivialis* occur at the top of the Gurpi Formation, still indicating the Danian (biozone P3, ca. 62 Ma).

The calcareous nannofossils *Prinsius martinii* and *Toweius pertusus* from the basal Amiran Formation indicate biozone CNP4–CNP5 (63–61 Ma, Danian–early Selandian). Planktonic foraminifera from intercalated limestones and marls of the Amiran Formation include *Globanomalina chapmani*, *Globanomalina ovalis*, *Eoglobigerina edita*, and *Morozovella acuta*, indicating biozone P4a (ca. 60 Ma, Selandian).

Abundant foraminiferal assemblages including *Dictyokathina simplex*, *Plumokathina lenticula*, *Chiloguembelina parallela*, and *Morozovella aequa* from the Taleh Zang Formation point at biozones P4b–P5a (60–56 Ma, late Selandian–Thanetian). Marker species of calcareous nannofossils were not identified in the Taleh Zang and Kashkan Formations, but sample 19AM208 from the base of the Kashkan Formation yielded larger benthic foraminifera *Orbitolites shirazensis*, *Lockhartia conditi*, and *Rotalia cf. newboldi* indicating biozone P5b (56–54.9 Ma, early Ypresian). Miocene ages are indicated for samples 19AM237–19AM243 from the Asmari Formation at the top of the section, yielding foraminifera *Dendritina rangi*, *Neorotalia lithothamnica*, and *Turborotalia pseudoampliapertura* (biozones P18–P19, 33.9–30.3 Ma).

PROVENANCE OF AMIRAN AND KASHKAN SANDSTONES

Detrital zircons from both the Amiran and Kashkan Formations show three similar Permo-

Samples 19AM01–19AM40 from the lower Gurpi Formation yielded Cretaceous planktonic foraminifera. The co-occurrence of *Radotruncana*

subspinoso, *Globotruncana aegyptiaca*, *Gansserina gansseri*, and *Pseudotextularia nuttalli* suggests an age not older than the late

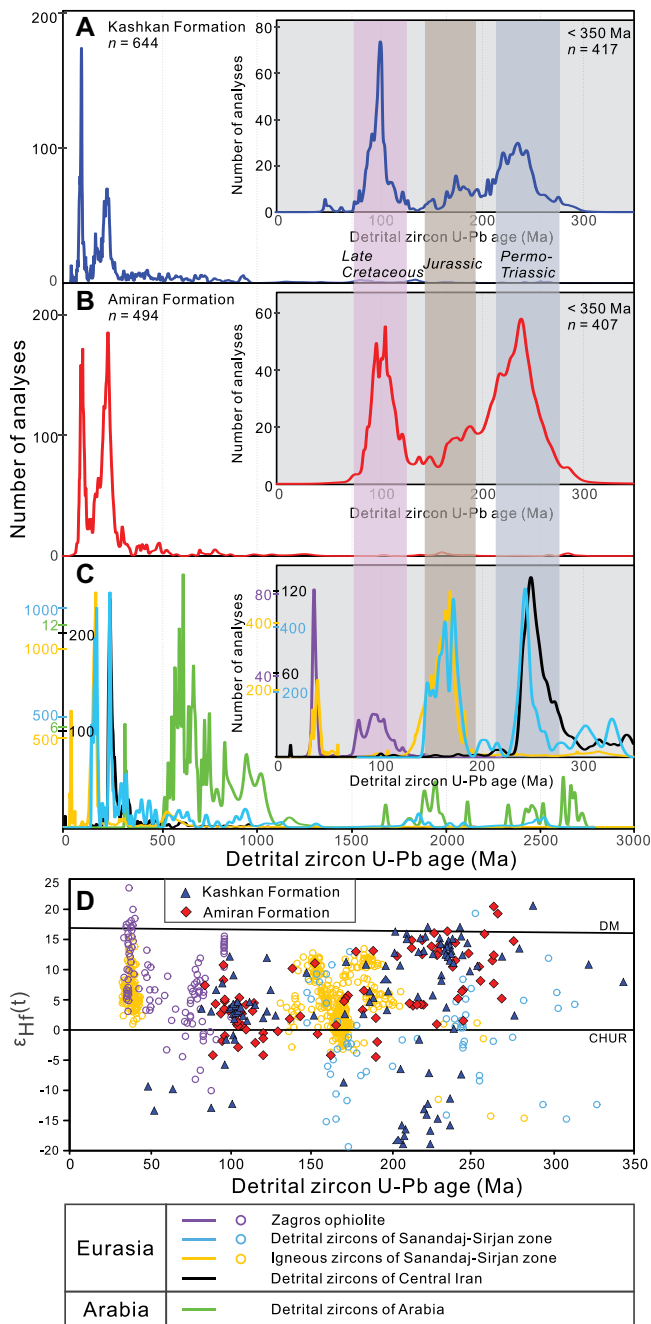


Figure 3. U-Pb age and Hf isotope data for detrital zircon in Kashkan (A, D) and Amiran sandstones (B, D) of this study, compared with potential source areas (C, D; data from Ao et al., 2016; Chiu et al., 2017; Zhang et al., 2017, 2018; Al Humadi et al., 2019; Barber et al., 2019; Meinhold et al., 2020; GholamiZadeh et al., 2022).

ter (Fig. 3C) but largely with different $\epsilon_{\text{Hf}}(t)$ values (GholamiZadeh et al., 2022; Fig. 3D). Some zircons yielding relatively high $\epsilon_{\text{Hf}}(t)$ values (from +9.5 to +20.4), relatively low U concentrations ($\sim 80\% < 200$ ppm and some even < 10 ppm), and homogeneous internal structures in CL images indicating crystallization from mafic magma were possibly derived from mid-ocean ridge-type Triassic Neotethyan oceanic crust (Barber et al., 2019). Zircon grains in Kashkan sandstones with relatively low $\epsilon_{\text{Hf}}(t)$ values (from -19.2 to -6.8) may have been part of recycled detritus from Central Iran (Fig. 3C; Meinhold et al., 2020), together with siltstone lithic fragments (Lp in Fig. 2) and pebbles identified during counting of conglomerate clasts ($\sim 5\%$; Fig. 2). Detrital zircons from Central Iran with similar age and Hf isotope characteristics have been reported from post-Miocene clastic rocks in the Zagros foreland basin (Zhang et al., 2017; Cai et al., 2021; GholamiZadeh et al., 2022). Age spectra of detrital zircons in Amiran and Kashkan sandstones testify that detritus from Eurasia was deposited onto Arabia by the beginning of the Eocene.

OPHIOLITE OBUCTION FOLLOWED BY ARABIA-EURASIA COLLISION

Provenance analysis provides new constraints on the paleogeographic and paleotectonic evolution of the Zagros orogen. The Kermanshah and other Zagros ophiolites were generated in supra-subduction settings during the early Late Cretaceous (Moghadam et al., 2022) and consequently obducted onto the passive continental margin of Arabia (Figs. 4A and 4C). Southward obduction of the Kermanshah ophiolite induced subsidence along the northeastern edge of the Arabian lower plate and formation of the Amiran foreland basin, where sediments of the Gurpi Formation accumulated in the Campanian–Maastrichtian. Exposure above sea level of the ophiolite resulted in progressively increasing ophioliticlastic supply, as documented by the upward-coarsening Paleocene Amiran Formation (ca. 64–60 Ma). To the north of the Kermanshah ophiolite, the Sanandaj-Sirjan zone also provided detritus to the deep-water Amiran Basin. Detritus from Central Iran was not yet documented at this stage.

Starting from the base of the Eocene (ca. 56 Ma; Figs. 4B and 4D), fluvio-deltaic sediments of the Kashkan Formation were deposited onto the shallow-water foraminiferal limestones of the Taleh Zang Formation (ca. 60–56 Ma). Provenance data indicate that the newly established, southward-flowing fluvial system originated from Central Iran, although most detritus reaching the Amiran Basin was still locally derived from erosion of the sub-aerial Kermanshah ophiolite. The deposition of the Kashkan Formation thus sealed the suture zone, demonstrating that continental collision

Triassic (260–200 Ma), Jurassic (180–160 Ma), and Cretaceous (~ 110 –80 Ma) age clusters, quite distinct from the dominant > 500 Ma age of detrital zircons derived from Arabia (Fig. 3). Cretaceous zircons with varied $\epsilon_{\text{Hf}}(t)$ values are consistent with the age of the Zagros ophiolite and related magmatic rocks (Ao et al., 2016; Al Humadi et al., 2019), indicating overwhelming supply from an obducted ophiolite complex (Garzanti et al., 2002), plausibly the Kermanshah ophiolite to the north (Moghadam and Stern, 2015; Ao et al., 2016). Ophiolite provenance is also confirmed by the occurrence of serpentinite rock fragments (Lv in Fig. 2) and Cr-spinel grains yielding relatively high Cr# [$100 \times \text{Cr}/(\text{Cr} + \text{Al})$], similar to those con-

tained in Zagros ophiolites (Fig. 2; Dick and Bullen, 1984; Moghadam and Stern, 2015). Jurassic (180–160 Ma) zircons with weakly negative to positive $\epsilon_{\text{Hf}}(t)$ values compare well with Jurassic igneous and detrital zircons in the Sanandaj-Sirjan zone (Fig. 3; Chiu et al., 2013, 2017; Hassanzadeh and Wernicke, 2016; Zhang et al., 2018), which may have supplied the few volcanic rock fragments contained in Amiran and Kashkan sandstones. The source of Permo-Triassic (260–200 Ma) zircons is harder to determine because only a few Permo-Triassic magmatic rocks are exposed in surrounding regions. Detrital zircons in Sanandaj-Sirjan zone sandstones do contain a similar age cluster as the Permo-Triassic zircons age clus-

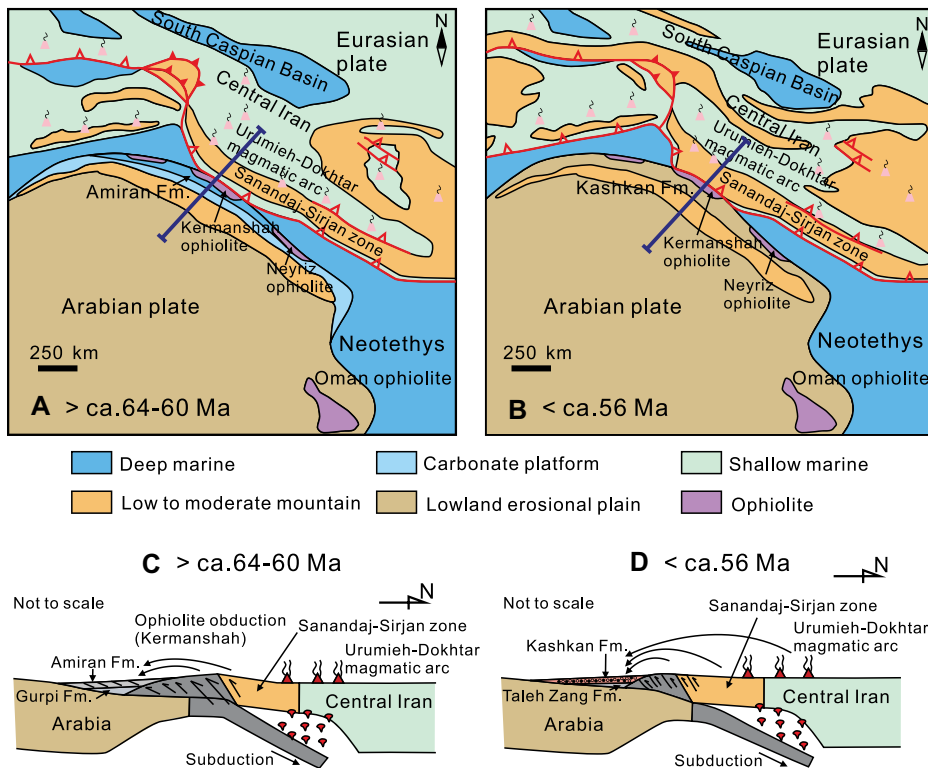


Figure 4. Paleocene to Eocene paleogeographic sketch maps (modified from Barrier et al., 2018) and schematic tectonic evolution along the Zagros belt.

between Arabia and Iran took place before the Eocene (i.e., before ca. 56 Ma) in the Lorestan region. This revised collision time is certified by the magmatic quiescence of ca. 72–57 Ma in the Urumieh-Dokhtar magmatic arc (Chiu et al., 2013). The subsequent magmatic flare-up (ca. 55–25 Ma) and early Eocene emplacement of adakitic rocks thus occurred during the crustal thickening and delamination stage in the syn- and post-collisional settings instead of the pre-collisional, oceanic subduction stage (Chiu et al., 2013; Mokhtari et al., 2022). Provenance analysis of sandstones deposited in Iraqi Kurdistan to the northwest and in the Fars-Neyriz region of Iran to the southeast failed to indicate evidence of continental collision between Arabia and Eurasia before ca. 36–26 Ma (Koshnaw et al., 2019; Cai et al., 2021; GholamiZadeh et al., 2022), which may be ascribed either to an incomplete sedimentary record or to diachronous collision starting earlier in the Amiran transect than in both the northwestern and southeastern segments of the Zagros orogen.

A pre-Eocene initiation of the Arabia-Eurasia collision matches what is documented for the India-Eurasia collision in the Himalaya and southern Tibet (Hu et al., 2015), implying that the Neotethys Ocean closed roughly synchronously from Tibet to the Zagros, which is of great significance for the understanding of the continental collision and plate-tectonic kinematics (e.g., Hatzfeld and Molnar, 2010).

CONCLUSIONS

New provenance data and age constraints from the Amiran Basin indicate that the obducted Kermanshah ophiolite was actively eroded in the Paleocene, as documented by ophioliticlastic detritus in the deep-marine Amiran Formation. The overlying fluvio-deltaic Kashkan Formation contains additional detritus from Central Iran, indicating that the closure of the Neotethys Ocean and consequent onset of the Arabia-Eurasia collision took place before the Eocene (i.e., before ca. 56 Ma).

ACKNOWLEDGMENTS

We are grateful to Mansour Ghorbani for logistical field assistance in Iran, and to Fuyuan Wu and Parisa GholamiZadeh for beneficial discussions. We thank William Clyde for editorial handling and Sunlin Chung, Kwan Nang Pang, and two anonymous reviewers for their constructive comments and suggestions. This study was financially supported by the National Natural Science Foundation of China (91755209 and 42072124).

REFERENCES CITED

- Agard, P., Omrani, J., Jolivet, L., Whitechurch, H., Vrielynck, B., Spakman, W., Monié, P., Meyer, B., and Wortel, R., 2011, Zagros orogeny: A subduction-dominated process: *Geological Magazine*, v. 148, p. 692–725, <https://doi.org/10.1017/S001675681100046X>.
- Agnini, C., Fornaciari, E., Raffi, I., Catanzariti, R., Pälke, H., Backman, J., and Rio, D., 2014, Biozonation and biochronology of Paleogene calcareous nannofossils from low and middle latitudes: *Newsletters on Stratigraphy*, v. 47, p. 131–181, <https://doi.org/10.1127/0078-0421/2014/0042>.

- Alavi, M., 1994, Tectonics of the Zagros orogenic belt of Iran: New data and interpretations: *Tectonophysics*, v. 229, p. 211–238, [https://doi.org/10.1016/0040-1951\(94\)90030-2](https://doi.org/10.1016/0040-1951(94)90030-2).
- Alavi, M., 2004, Regional stratigraphy of the Zagros fold-thrust belt of Iran and its foreland evolution: *American Journal of Science*, v. 304, p. 1–20, <https://doi.org/10.2475/ajs.304.1.1>.
- Al Humadi, H., Väisänen, M., Ismail, S.A., Kara, J., O'Brien, H., Lahaye, Y., and Lehtonen, M., 2019, U-Pb geochronology and Hf isotope data from the Late Cretaceous Mawat ophiolite, NE Iraq: *Heliyon*, v. 5, <https://doi.org/10.1016/j.heliyon.2019.e02721>.
- Ao, S.J., Xiao, W.J., Khalatbari Jafari, M., Talebian, M., Chen, L., Wan, B., Ji, W.Q., and Zhang, Z.Y., 2016, U-Pb zircon ages, field geology and geochemistry of the Kermanshah ophiolite (Iran): From continental rifting at 79 Ma to oceanic core complex at ca. 36 Ma in the southern Neo-Tethys: *Gondwana Research*, v. 31, p. 305–318, <https://doi.org/10.1016/j.gr.2015.01.014>.
- Barber, D.E., Stockli, D.F., and Galster, F., 2019, The Proto-Zagros foreland basin in Lorestan, western Iran—Insights from multi-mineral detrital geo-thermochronometric and trace-elemental provenance analysis: *Geochimica et Geophysica*, v. 20, p. 2657–2680, <https://doi.org/10.1029/2019GC008185>.
- Barrier, E., Vrielynck, B., Brouillet, J.-F., and Brunet, M.-F., 2018, Paleotectonic reconstruction of the central Tethyan Realm: *Tectono-Sedimentary-Palinspastic maps from late Permian to Pliocene*: Paris, Commission for the Geological Map of the World, atlas of 20 maps, scale 1:15,000,000.
- BouDagher-Fadel, M.K., 2018, Revised diagnostic first and last occurrences of Mesozoic and Cenozoic planktonic foraminifera: University College London Office of the Vice-Provost Research Professional Paper 2, p. 1–5, <https://discovery.ucl.ac.uk/id/eprint/10048262>.
- Cai, F.L., et al., 2021, Configuration and timing of collision between Arabia and Eurasia in the Zagros collision zone, Fars, southern Iran: *Tectonics*, v. 40, <https://doi.org/10.1029/2021TC006762>.
- Chiu, H.Y., Chung, S.L., Zarrinkoub, M.H., Mohammadi, S.S., Khatib, M.M., and Izuka, Y., 2013, Zircon U-Pb age constraints from Iran on the magmatic evolution related to Neotethyan subduction and Zagros orogeny: *Lithos*, v. 162–163, p. 70–87, <https://doi.org/10.1016/j.lithos.2013.01.006>.
- Chiu, H.Y., Chung, S.L., Zarrinkoub, M.H., Melkonyan, R., Pang, K.N., Lee, H.Y., Wang, K.L., Mohammadi, S.S., and Khatib, M.M., 2017, Zircon Hf isotopic constraints on magmatic and tectonic evolution in Iran: Implications for crustal growth in the Tethyan orogenic belt: *Journal of Asian Earth Sciences*, v. 145, p. 652–669, <https://doi.org/10.1016/j.jseas.2017.06.011>.
- Dick, H.J.B., and Bullen, T., 1984, Chromian spinel as a petrogenetic indicator in abyssal and alpine-type peridotites and spatially associated lavas: *Contributions to Mineralogy and Petrology*, v. 86, p. 54–76, <https://doi.org/10.1007/BF00373711>.
- Garzanti, E., Vezzoli, G., and Andò, S., 2002, Modern sand from obducted ophiolite belts (Sultanate of Oman and United Arab Emirates): *The Journal of Geology*, v. 110, p. 371–391, <https://doi.org/10.1086/340440>.
- GholamiZadeh, P., Hu, X.M., Garzanti, E., and Adabi, M.H., 2022, Constraining the timing of Arabia-Eurasia collision in the Zagros orogen by sandstone provenance (Neyriz, Iran): *Geological Society of America Bulletin*, v. 134, p. 1793–1810, <https://doi.org/10.1130/B35950.1>.
- Hassanzadeh, J., and Wernicke, B.P., 2016, The Neotethyan Sanandaj-Sirjan zone of Iran as an ar-

- chetype for passive margin–arc transitions: *Tectonics*, v. 35, p. 586–621, <https://doi.org/10.1002/2015TC003926>.
- Hatzfeld, D., and Molnar, P., 2010, Comparisons of the kinematics and deep structures of the Zagros and Himalaya and of the Iranian and Tibetan plateaus and geodynamic implications: *Reviews of Geophysics*, v. 48, RG2005, <https://doi.org/10.1029/2009RG000304>.
- Homke, S., Vergés, J., Serra-Kiel, J., Bernaola, G., Sharp, I., Garcés, M., Montero-Verdú, I., Karpuz, R., and Goodarzi, M.H., 2009, Late Cretaceous–Paleocene formation of the proto-Zagros foreland basin, Lorestan Province, SW Iran: *Geological Society of America Bulletin*, v. 121, p. 963–978, <https://doi.org/10.1130/B26035.1>.
- Hu, X.M., Garzanti, E., Moore, T., and Raffi, I., 2015, Direct stratigraphic dating of India–Asia collision onset at the Selandian (middle Paleocene, 59 ± 1 Ma): *Geology*, v. 43, p. 859–862, <https://doi.org/10.1130/G36872.1>.
- Huber, B.T., Petrizzo, M.R., Young, J.R.E., Falzoni, F., Gilardoni, S.E., Bown, P.R., and Wade, B.S., 2016, Pforams@mikrotax: A new online taxonomic database for planktonic foraminifera: *Micropaleontology*, v. 62, p. 429–438, <https://www.jstor.org/stable/26645533>, <https://doi.org/10.47894/mpal.62.6.02>.
- Ingersoll, R.V., Fullard, T.F., Ford, R.L., Grimm, J.P., Pickle, J.D., and Sares, S.W., 1984, The effect of grain size on detrital modes: A test of the Gazzi–Dickinson point-counting method: *Journal of Sedimentary Research*, v. 54, p. 103–116, <https://doi.org/10.1306/212F83B9-2B24-11D7-8648000102C1865D>.
- Koshnaw, R.I., Stockli, D.F., and Schlunegger, F., 2019, Timing of the Arabia–Eurasia continental collision—Evidence from detrital zircon U–Pb geochronology of the Red Bed Series strata of the northwest Zagros hinterland, Kurdistan region of Iraq: *Geology*, v. 47, p. 47–50, <https://doi.org/10.1130/G45499.1>.
- Koshnaw, R.I., Schlunegger, F., and Stockli, D.F., 2021, Detrital zircon provenance record of the Zagros mountain building from the Neotethys obduction to the Arabia–Eurasia collision, NW Zagros fold–thrust belt, Kurdistan region of Iraq: *Solid Earth*, v. 12, p. 2479–2501, <https://doi.org/10.5194/se-12-2479-2021>.
- McQuarrie, N., and van Hinsbergen, D.J.J., 2013, Retrodeforming the Arabia–Eurasia collision zone: Age of collision versus magnitude of continental subduction: *Geology*, v. 41, p. 315–318, <https://doi.org/10.1130/G33591.1>.
- Meinhold, G., Azizi, S.H.H., and Berndt, J., 2020, Permian–Triassic magmatism in response to Palaeotethys subduction and pre-Late Triassic arrival of northeast Gondwana-derived continental fragments at the southern Eurasian margin: Detrital zircon evidence from Triassic sandstones of Central Iran: *Gondwana Research*, v. 83, p. 118–131, <https://doi.org/10.1016/j.gr.2020.02.001>.
- Moghadam, H.S., and Stern, R.J., 2015, Ophiolites of Iran: Keys to understanding the tectonic evolution of SW Asia: (II) Mesozoic ophiolites: *Journal of Asian Earth Sciences*, v. 100, p. 31–59, <https://doi.org/10.1016/j.jseas.2014.12.016>.
- Moghadam, H.S., Li, Q.L., Griffin, W.L., Chiaradia, M., Hoernle, K., O’Reilly, S.Y., and Esmaeili, R., 2022, The Middle-Late Cretaceous Zagros ophiolites, Iran: Linking of a 3000 km swath of subduction initiation fore-arc lithosphere from Troodos, Cyprus to Oman: *Geological Society of America Bulletin*, v. 134, p. 1414–1442, <https://doi.org/10.1130/B36041.1>.
- Mokhtari, M.A.A., Kouhestani, H., Pang, K.N., Chung, S.L., Lee, H.Y., and Hsu, S.C., 2022, Early Eocene high-Sr/Y magmas from the Urumieh–Dokhtar paleo-arc, Iran: Implications for the origin of high-flux events in magmatic arcs: *Lithos*, v. 416–417, <https://doi.org/10.1016/j.lithos.2022.106656>.
- Pirouz, M., Avouac, J.-P., Hassanzadeh, J., Kirschvink, J.L., and Bahroudi, A., 2017, Early Neogene foreland of the Zagros, implications for the initial closure of the Neo-Tethys and kinematics of crustal shortening: *Earth and Planetary Science Letters*, v. 477, p. 168–182, <https://doi.org/10.1016/j.epsl.2017.07.046>.
- Saura, E., et al., 2011, Basin architecture and growth folding of the NW Zagros early foreland basin during the Late Cretaceous and early Tertiary: *Journal of the Geological Society*, v. 168, p. 235–250, <https://doi.org/10.1144/0016-76492010-092>.
- Takin, M., Akbari, Y., and Macleod, J.H., 1970, Pul-e-Dukhtar. Geological Complication Map: Geological and Exploration Division, Iranian Oil Operating Companies, Tehran, scale: 1:100,000.
- Zhang, Z.Y., Xiao, W.J., Majidifard, M.R., Zhu, R.X., Wan, B., Ao, S.J., Chen, L., Rezaeian, M., and Esmaeili, R., 2017, Detrital zircon provenance analysis in the Zagros Orogen, SW Iran: Implications for the amalgamation history of the Neo-Tethys: *International Journal of Earth Sciences*, v. 106, p. 1223–1238, <https://doi.org/10.1007/s00531-016-1314-3>.
- Zhang, Z.Y., et al., 2018, Geochemistry, zircon U–Pb and Hf isotope for granitoids, NW Sanandaj–Sirjan zone, Iran: Implications for Mesozoic–Cenozoic episodic magmatism during Neo-Tethyan lithospheric subduction: *Gondwana Research*, v. 62, p. 227–245, <https://doi.org/10.1016/j.gr.2018.04.002>, corrigendum available at <https://doi.org/10.1016/j.gr.2018.09.001>.

Printed in the USA